[AMERICAN JOURNAL OF SCIENCE, VOL. 282, APRIL, 1982, P. 512-541]

AN IDEALIZED MODEL OF NITROGEN RECYCLING IN MARINE SEDIMENTS

G. BILLEN

Laboratoire d'Océanographie, University of Brussels,
Brussels, Belgium

ABSTRACT. A model of the interdependent processes involved in nitrogen mineralization in marine sediments is presented, based on data collected in the sandy sediments of the North Sea. It relates the flux of organic material deposited in the sediments to the release of dissolved nitrogen to the overlying water, given the mixing conditions undergone by the solid and interstitial phases of the sediment under the action of physical or biological processes.

Although idealized, the model can be useful in predicting the trends of variation in the relative importance of ammonification, nitrification, and denitrification, as a result of variations in the organic matter input to the bottom. It shows that, at low input of organic matter, most nitrogen release occurs as nitrate, whereas, at higher input, ammonium release prevails. Denitrification reaches a plateau above a certain input of organic material. It can involve an appreciable proportion (more than about 30 percent of the flux) of remineralized nitrogen only at high organic input and when a high nitrate concentration exists in the overlying water.

INTRODUCTION

In the framework of overall ecological models of aquatic ecosystems, the sediments are often viewed as a black box which behaves with respect to the water column as a sink for organic material and as a source of dissolved nutrients. Usually the flux of nutrients from the sediment has been parameterized and not calculated as a part of the model (for example, Pichot, ms).

Experimental methods have been developed for determining the flux of nutrients across the sediment-water interface. Some of these methods involve direct measurement of the accumulation rate of nutrients in the overlying water, either in bell-jars deposited on the bottom or in the top of a freshly collected core (for example, Fanning and Pilson, 1974; Rowe and others, 1975). Other authors have developed diagenetic models for describing the vertical concentration profiles of various chemical species either in the solid phase or in the pore water of sediments (Berner, 1964, 1971, 1974, 1980a; Imboden, 1975; Lerman, 1979; and others). Such models allow the vertical distribution of chemical substances within the sediments to be related to the rates of the physical, chemical, or biological processes affecting them. When used in combination with direct measurements of microbial activities, they provide the information needed for making up a balance of nutrient recycling in the sediments (Billen, 1978). This last method involves a complete description of the processes responsible for nutrient remineralization, so that it can be the basis of a comprehensive model relating the rates of nutrient release to the input of organic material deposited in the sediments.

Based mainly on data collected from the sediments of the North Sea (Billen, 1978), this paper presents an idealized model of nitrogen recycling in sediments taking into account the redox conditions prevailing in them.

SYMBOLS NOMENCLATURE AND DIMENSIONS

a_0	ammonification rate in the upper layer of the sediment (mass • volume^{-1} • time^{-1})
c_j	consumption rate of oxidant j (mass • volume^{-1} • time^{-1})
$C_{orgC/N}$	concentration of organic carbon nitrogen (mass • volume^{-1})
$C^0_{orgC/N}$	concentration of organic carbon nitrogen in the upper layer of the sediment (mass • volume^{-1})
C_{NO_3}, C_{NH_4}	concentration of dissolved nitrate or ammonium in the sediment (mass • volume^{-1})
$C^0_{NO_3}$, $C^0_{NH_4}$	concentration of nitrate of ammonium in the overlying water (mass • volume^{-1})
C_{Ox_j}	concentration of oxidant j (mass • volume^{-1})
D_s	dispersion coefficient for the solid phase (surface • time^{-1})
D_i	dispersion coefficient for the interstitial phase (surface • time^{-1})
Eh	redox potential (Volt)
$J^0_{NO_3}$, $J^0_{NH_4}$, J^0_{org}	flux of nitrate, ammonium, or organic matter across the sediment water interface. Positive when directed downward (mass • surface^{-1} • time^{-1})
k_a	first order constant of organic matter degradation (time^{-1})
k_d	first order constant of denitrification (time^{-1})
k_n	rate of nitrification (mass • volume^{-1} • time^{-1})
k^0_n	rate of nitrification in the upper layer of the sediment (mass • volume^{-1} • time^{-1})
m_{Ox_j}	molar concentration of oxidant j (mole • kg solvent^{-1})
p_j	production rate of oxidant j (mass • volume^{-1} • time^{-1})
$R(z)$	rate of organic carbon degradation (mass • volume^{-1} • time^{-1})
t	time
z	depth
z_n	depth of the nitrification layer
α	$= \sqrt{\frac{k_a}{D_s}}$ (length^{-1})
β	C/N ratio of organic matter in sediments (dimensionless)
γ	proportionality coefficient between nitrification rate and ammonification rate (dimensionless)

ϵ step function equal to zero for $z \geqslant z_n$
1 for $z < z_n$

ν_j number of equivalent per mole of oxidant j

ϕ porosity of the sediment (mass pore water per unit volume sediment)

INTERDEPENDENT DIAGENETIC MODELS FOR ORGANIC CARBON, ORGANIC NITROGEN, AMMONIUM, AND NITRATE

I shall briefly summarize here the diagenetic equations that can be used for describing organic carbon, organic nitrogen, ammonium, and nitrate concentration profiles, in shallow sandy sediments such as those of the North Sea, emphasizing the interdependences between the behavior of these four species.

The vertical profiles of organic carbon and organic nitrogen can be simulated by the solution of the differential equations expressing at each depth the mass balance of particulate organic material under the effect of bacterial degradation and solid phase mixing. Advection due to sediment accumulation can be neglected in the case of the sandy sediments of the North Sea where deposition rates are very low (about 0.03 cm/yr as a mean according to McCave, 1973). Mixing of the solid phase due to bioturbation and recurrent resuspension is taken into account considering an apparent Fickian-like mixing coefficient D_s.

Due to poor knowledge of the mechanisms of the rate-limiting steps of organic matter degradation in natural environments, it is customary to assume that the rate of the overall process is first order with respect to organic matter. For taking into account the different susceptibilities to bacterial attack of different classes of compounds making up the overall organic matter, Jørgensen (1978) and Berner (1980a, b) have suggested the use of "multi-G's-first order kinetics", in which each particular class of organic matter is assumed to be degraded according to its own first order constant, k_i. A simplified approach will be used here, considering organic material as made of only two classes: a non-biodegradable fraction with zero k, and a biodegradable fraction, with a measurable first-order degradation kinetic constant, which will be considered as being independent of depth (at least in the uppermost few centimeters) and of the microbiological process of degradation.

This leads to the following diagenetic equation:

$$\frac{\partial C_{org}}{\partial t} = D_s \frac{\partial^2 C_{org}}{\partial z^2} - k_a C_{org} \qquad (1)$$

where C_{org} is the biodegradable organic carbon or nitrogen concentration expressed per unit sediment volume,

k_a is the first order kinetic constant of organic matter degradation,

z is the depth,

t is the time,

and D_s is the solid phase mixing coefficient.

Considering the following boundary conditions:

$$C_{org} = C^{\circ}_{org} \qquad \text{for } z = 0$$

$$C_{org} \text{ asymptotes to zero for } z = \infty$$

the stationary solution ($\partial c/\partial t = 0$) of eq (1) is

$$C_{org} = C^{\circ}_{org}\, e^{-\alpha z} \tag{2}$$

with

$$\alpha = \sqrt{\frac{k_a}{D_s}}$$

The flux of sedimenting organic material (J°_{org}) can be calculated by the following relation:

$$J^{\circ}_{org} = -D_s \left[\frac{dC_{org}}{dz}\right]_{z=0} = D_s \cdot \alpha C^{\circ}_{org} \tag{3}$$

while the integrated rate of organic matter degradation (I_{org}) is given by:

$$I_{org} = \int_0^{\infty} k_a C_{org} dz = \frac{k_a}{\alpha} C^{\circ}_{org} \tag{4}$$

These relations are assumed to hold either for organic carbon or organic nitrogen. For the sake of simplicity, we will ignore here the preferential degradation of nitrogen rich organic compounds by microorganisms resulting in an increase of the C/N ratio of degrading organic matter with depth in the sediment (Aller and Yingst, 1980; Rosenfeld, 1981). Thus k_a will be assumed to be the same for carbon and nitrogen remineralization, and the C/N ratio of biodegradable organic matter (β) is supposed constant in the depth interval considered.

Mathematical simulation of the vertical distribution of nitrate concentration in interstitial water of marine sediments with nitrification and denitrification has been discussed in detail by Vanderborght and Billen (1975). They suggested the following diagenetic equation, again neglecting sedimentation.

$$\frac{\partial C_{NO_3}}{\partial t} = D_i \frac{\partial^2 C_{NO_3}}{\partial z^2} + \epsilon k_n - (1-\epsilon) k_d C_{NO_3} \tag{5}$$

with

$\epsilon = 1$ for $z \leqslant z_n$ (nitrification layer)

$\epsilon = 0$ for $z \geqslant z_n$ (denitrification layer).

C_{NO_3} is the nitrate concentration expressed per unit sediment volume,

D_i is the dispersion coefficient for dissolved species in the sediment,

k_n is the mean rate of nitrification within the nitrification layer,

k_d is the first order rate constant of denitrification with respect to nitrate.

In sandy sediments, porosity changes with depth are negligible; in any case, they are implicitly taken into account in eq (5) by considering the concentration expressed by unit sediment volume instead of by unit pore water volume.

The stationary solution of eq (5), with the following boundary conditions:

$$C_{NO_3} = C°_{NO_3} \text{ for } z = 0$$

$$\left.\begin{aligned} &[C_{NO_3}]_{\text{nitrification layer}} = [C_{NO_3}]_{\text{denitrification layer}} \\ &\left[\frac{dC_{NO_3}}{dz}\right]_{\text{nitrification layer}} = \left[\frac{dC_{NO_3}}{dz}\right]_{\text{denitrification layer}} \end{aligned}\right\} \text{ for } z = z_n$$

$$C_{NO_3} \text{ finite for } z = \infty$$

is:

$$\left.\begin{aligned} C_{NO_3} &= -\frac{k_n}{2D_i} z^2 + \left[\frac{[k_n/D_i]\left[\frac{1}{2} z^2_n + \sqrt{D_i/k_d}\, z_n\right] - C°_{NO_3}}{z_n + \sqrt{D_i/k_d}}\right] z + C°_{NO_3} && \text{for } z \leqslant z_n \\ C_{NO_3} &= C_{NO_3\,(z=z_n)} \exp\left[-\sqrt{k_d/D_i}\,(z - z_n)\right] && \text{for } z \geqslant z_n \end{aligned}\right\} \quad (6)$$

where $C°_{NO_3}$ is the nitrate concentration in the overlying water.

The flux of nitrate across the sediment-water interface ($J°_{NO_3}$) is given by:

$$J°_{NO_3} = -D_i \left[\frac{dC_{NO_3}}{dz}\right]_{z=0} = -D_i \frac{\frac{k_n}{D_i}\left[\frac{z_n^2}{2} + \sqrt{\frac{D_i}{k_d}}\, z_n\right] - C°_{NO_3}}{z_n + \sqrt{\frac{D_i}{k_d}}} \quad (7)$$

while the integrated rate of nitrification (I_{nitr}) is given by:

$$I_{nitr} = \int_0^{z_n} k_n \cdot dz = k_n\, z_n \quad (8)$$

and the integrated rate of denitrification (I_{denitr}), equal to the flux of nitrate diffusing from the nitrification layer to the denitrification layer is given by

$$\begin{aligned} I_{denitr} &= \int_{z_n}^{\infty} k_d\, C_{NO_3}\, dz = -D_i \left[\frac{dC_{NO_3}}{dz}\right] z = z_n \\ &= + k_n\, z_n - \frac{k_n \left(\frac{z_n^2}{z} + \sqrt{\frac{D_i}{k_d}}\, z_n\right) - D_i C°_{NO_3}}{z_n + \sqrt{\frac{D_i}{k_d}}} \end{aligned} \quad (9)$$

The diagenetic equation for ammonium concentration can now be written in the following way, considering dispersion in the pore water, production by ammonification, and consumption by nitrification in the nitrification layer, and neglecting adsorption which is of limited importance in sandy sediments:

$$\frac{\partial C_{NH_4}}{\partial t} = D_i \frac{\partial^2 C_{NH_4}}{\partial z^2} + k_a C^\circ_{orgN} e^{-\alpha z} - \epsilon k_n \tag{10}$$

where k_a, C°_{orgN}, α, D_i, k_n, and ϵ have the same meaning as above.

With the following boundary conditions:

$C_{NH_4} = 0$ for $z = 0$

$$\left.\begin{aligned} &[C_{NH_4}]_{\text{nitrification layer}} = [C_{NH_4}]_{\text{denitrification layer}} \\ &\left[\frac{dC_{NH_4}}{dz}\right]_{\text{nitrification layer}} = \frac{dC_{NH_4}}{dz}_{\text{denitrification layer}} \end{aligned}\right\} z = z_n$$

C_{NH_4} remains finite for $z = \infty$

The stationary solution of eq (10) is

$$\begin{aligned} C_{NH_4} &= \frac{a_o}{\alpha^2 D_i}[1 - e^{-\alpha z}] + \frac{k_n}{2D_i}[z - 2z_n]z \qquad \text{for } z \leqslant z_n \\ C_{NH_4} &= \frac{a_o}{\alpha^2 D_i}[1 - e^{-\alpha z}] - \frac{k_n}{2D_i} z_n^2 \qquad \text{for } z \geqslant z_n \end{aligned} \tag{11}$$

with $a_o = k_a C^\circ_{orgN}$

The coherence of these models can be tested by using them for the simulation of the concentration profiles of particulate organic nitrogen, dissolved ammonium, and nitrate measured in June 1974 in a core of sandy sediments from the Southern Bight of the North Sea at station M 06 (51°28′30″N, 3°09′20″E) (fig. 1A).

If a concentration of about 20 μmoles N cm^{-3} is considered as corresponding to non-biodegradable organic nitrogen (asymptotic concentration), the organic nitrogen profile can be satisfactorily simulated by eq (2) for α in the range of 0.25 to 0.45 cm^{-1} (fig. 1B). An experimental value for the ammonium production rate in the topmost cm of sediment (a.) was determined to be 2.1×10^{-6} μmoles per cm^3 per second, by following ammonium concentration in a freshly collected sediment sample incubated at in situ temperature (14°C) and treated with a specific inhibitor of nitrification (fig. 2). Considering the mean organic nitrogen concentration in this layer (105 μmoles N cm^{-3}), the value of k_a can be calculated as 2×10^{-8} sec^{-1}. D_s can be evaluated from α to be in the range 1 to 3×10^{-7} cm^2 sec^{-1}.

The nitrification rate (k_n), determined by the ^{14}C-bicarbonate method of Billen (1976), was found to be about 0.5×10^{-6} μmoles N cm^3 sec^{-1} in

the upper 5 cm layer of this sediment. By adjustment of eq (6) to the experimental nitrate profile, the depth of the nitrification layer, z_n, was evaluated to be 7 cm, the dispersion coefficient, D_i, 8.5×10^{-5} cm^2 sec^{-1}, and the denitrification rate constant, 5×10^{-6} sec^{-1} (fig. 1B).

The simulation of the ammonium profile must now be obtained with the values of the parameters used for simulating the organic nitrogen and the nitrate profiles. When k_a, $C_{orgN}(°)$, D_i and k_n are fixed at the values determined above, the shape of the calculated profile is very sensitive to the value of α (fig. 1B). A very good fit of the experimental profile is obtained, however, for $\alpha = 0.375$, a value just in the middle of the range suggested by the organic nitrogen profile.

This indicates the consistency of our experimental data and of the model used for simulating them.

This model now allows an overall balance of nitrogen transformations to be made up for the particular sediment under study, using relations (3), (4), (7), (8), and (9), and the values of the parameters determined either by direct measurement or by adjustment. The results, presented diagramatically in figure 3, show that, from the total input of sedimenting organic nitrogen (5.6×10^{-6} μmoles N cm^{-2} sec^{-1}), about 20 percent is lost as N_2 or N_2O by denitrification, while the rest is recycled to the water column as ammonium (37 percent) or as nitrate (43 percent).

DERIVATION OF A GENERAL MODEL OF NITROGEN REMINERALIZATION

The model discussed in the preceding section has been developed with the object of applying it to a special sedimentary situation for which experimental data were available. It involves seven parameters (k_a, $C°_{orgN}$, D_s, D_i, k_n, z_n, k_d), two of which have been determined experimentally, the others by adjustment.

My purpose is now to work out a general a priori model of nitrogen recycling in sandy sediment, by modifying the preceding particular one,

Fig. 1

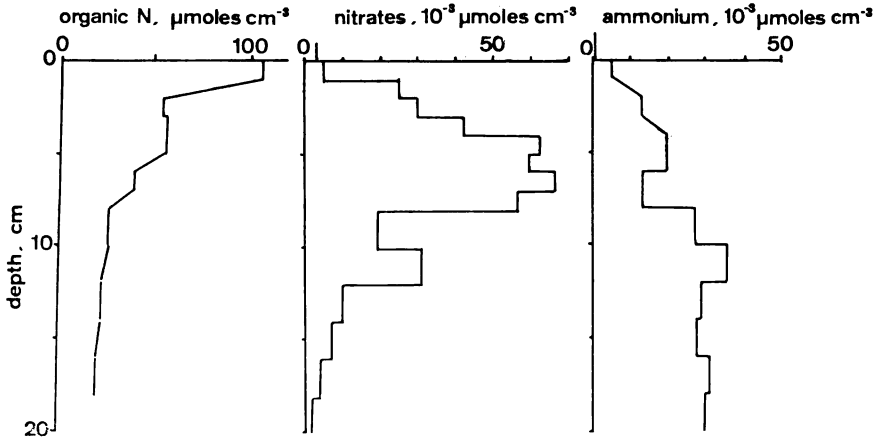

(A) Measured vertical profiles of nitrogen species in the sediments of station MO6 (51°28'30"N, 3°09'20"E) in the Southern Bight of the North Sea.

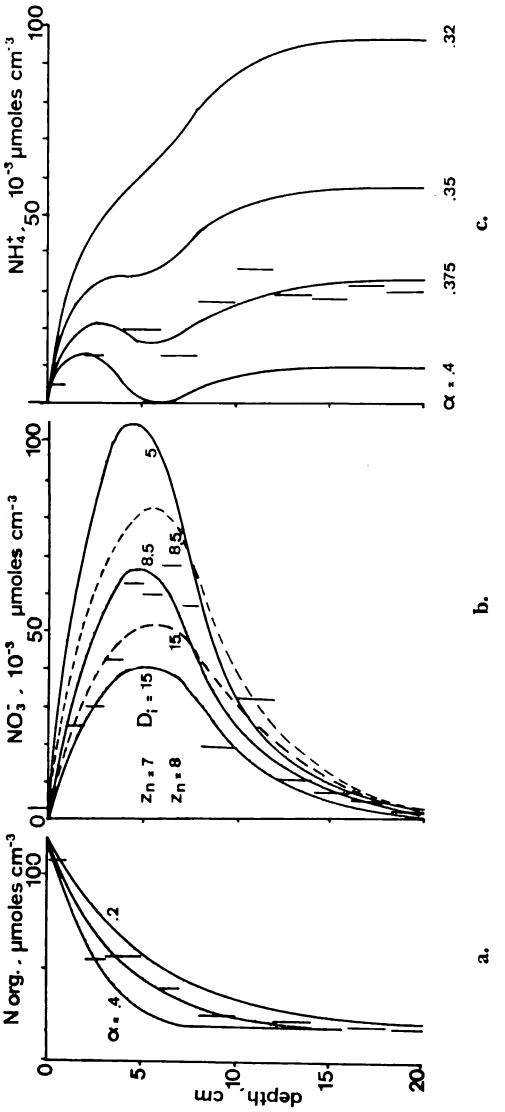

(B) Calculated vertical profiles of nitrogen species in sediments as compared with the experimental data of (A): (a) organic nitrogen: C_{Norg} (0) = 100 µmoles cm^{-3}, α = 0.2, 0.3, 0.4 cm^{-1}; (b) nitrate: k_n = 0.5 10^{-6} µmoles cm^{-3} sec^{-1}, z_n = 7 cm (solid line), 8 cm (broken line), kd = 5.3 10^{-6} sec^{-1}, D_1 = 10, 8.5, 5 10^{-6} cm^2 sec^{-1}; (c) ammonium: a_0 = 2.1 10^{-6} µmoles cm^{-3} sec^{-1}, α = 0.4, 0.375, 0.32 cm^{-1}

in order to relate the input of organic material deposited in the sediment to the release of dissolved nitrogen to the overlying water, given some abiotic characteristics of the sedimentary environment.

In such a model, the flux of depositing organic matter will be considered as the independent variable, while physical parameters, like D_i and D_s, will be considered as characterizing the abiotic environment. The interrelations between the five other "biotic" parameters must be further investigated, along with their dependence on environmental conditions.

Mixing and Dispersion Coefficients

The values of D_s and D_i characterize the overall mixing conditions undergone by the solid and interstitial phases of the sediment respectively, under the action of physical (currents, wave action . . .) or biological (bioturbation, irrigation . . .) processes.

Some values reported in the literature for these parameters in various near-shore aquatic environments are listed in table 1. In general, they agree with the values for sandy sediment of the North Sea found above. However, an important difference exists between the data from muddy and sandy sediments. High mixing coefficients for both the solid and interstitial phases of the sediment exist down to at least 15 cm in sands, whereas they are generally restricted to a few centimeters in muds. In the latter case, the sediment must be considered as made of two layers: a per-

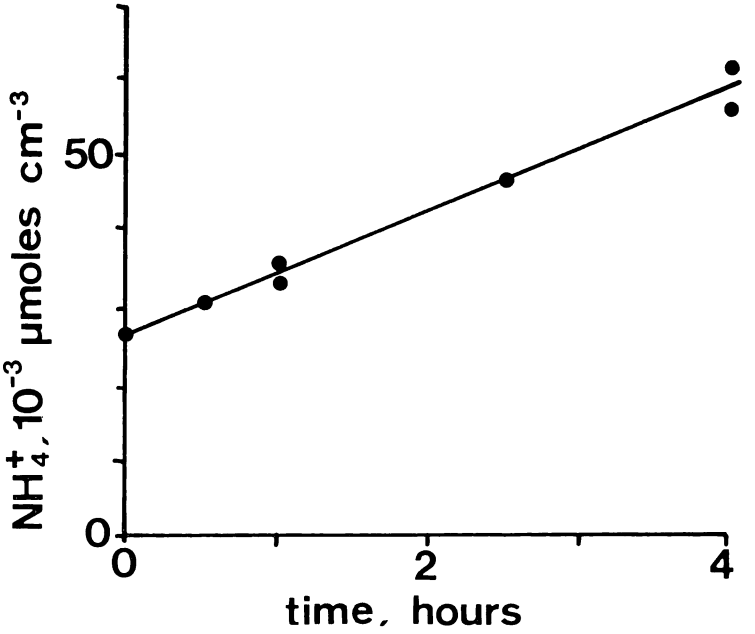

Fig. 2. Evolution of ammonium concentration in the interstitial water of a sample of the top sediment layer from station MO6, treated with N-serve and incubated at in situ temperature.

TABLE 1

Values of apparent vertical dispersion coefficient for the solid phase $D_s(a)$ or the interstitial phase $D_i(b)$ as determined in the upper layer of natural sediments by various authors

Location	Sediment type	Depth cm	D ($cm^2 sec^{-1}$)	Authors
A. Solid particles mixing (Ds)				
Chesapeake Bay	—	—	10^{-6}	Duursma and Gross, 1971
Buzzards Bay	—	0- 2	$3\ 10^{-8}$	Guinasso and Schink, 1975
Long Island Sound	mud	0- 2	$2\ 10^{-7}$	
Barnstable Harbor	—	0- 6	$0.8\ 10^{-7}$	
Holy Island Sands	sand	0-38	$4\ 10^{-5}$	
Caves Haven	sand	0-38	$0.7\ 10^{-5}$	
Fresh water Lake	mud	0- 6	$4.4\ 10^{-5}$	
Narragansett Bay	mud	0- 5	$3\ 10^{-7}$	Luedtke and Bender, 1979
Long Island Sound	mud	0- 4	$1.2\text{-}3.5\ 10^{-6}$	Aller and Cochran, 1976
Long Island Sound	mud	0- 5	$0.2\text{-}1.6\ 10^{-6}$	Aller and Yingst, 1980
Long Island Sound	mud	0- 4	$1.3\ 10^{-7}$	Krishnaswami and others, 1980
Lake Huron	mud	0-3/6	$1.2\ 10^{-7}$	Robbins, Krezoski, and Mozley, 1977
Coastal North Sea	sand	0-15	$1.4\ 10^{-7}$	Billen, this work
B. Pore water mixing (Di)				
Long Island Sound	mud	0- 8	$>2.8\ 10^{-6}$	Goldhaber and others, 1977
Coastal North Sea	mud	0-3.5	10^{-4}	Vanderborght, Wollast, and Billen, 1977
Coastal North Sea	sand	0->15	$0.5\text{-}2\ 10^{-4}$	Billen, 1978
Narragansett Bay	mud	0-25	$4\ 10^{-6}$	McCaffrey and others, 1980
Laboratory experiments	silt clay (with added Yoldia)	0- 4	10^{-6}	Aller, 1978
	(with added Clymenella)	0->11	$2.3\ 10^{-4}$	

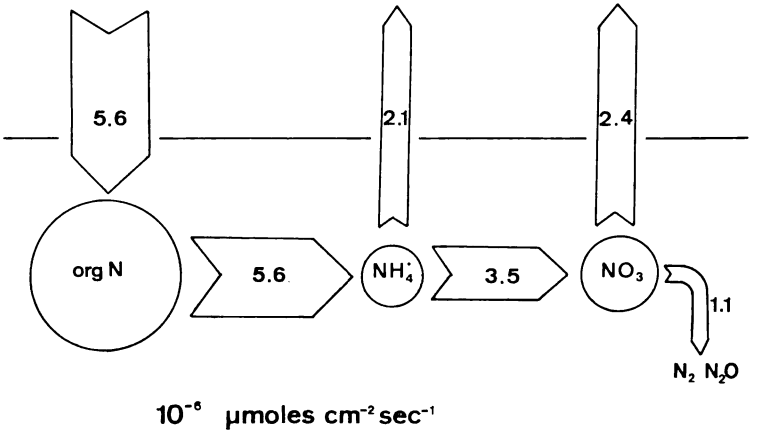

Fig. 3. Calculated balance of nitrogen transformation in the sediments at station MO6 of the Southern Bight of the North Sea.

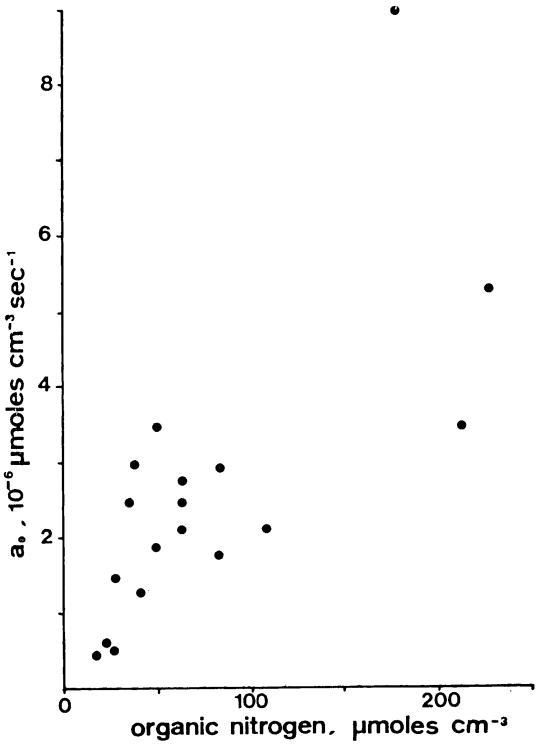

Fig. 4. Ammonification rate as a function of organic nitrogen content in the top layer of the sediments from the Southern Bight of the North Sea.

turbated upper layer where rapid mixing occurs, underlain by a deeper unmixed layer, where only molecular diffusion is responsible for the transport of dissolved species (Goldberg and Koide, 1962; Berger and Heath, 1968; Guinasso and Schink, 1975; Nozaki, Cochran, and Turekian, 1977; Vanderborght, Wollast, and Billen, 1977).

Ammonification Rate

In the preceding diagenetic model, the rate of ammonification has been considered as first order with respect to organic nitrogen content. This assumption can be checked on basis of direct determination of ammonification rates in the bottom sediments of the North Sea (Billen, 1978). When plotted against the organic nitrogen content in the upper layer of the corresponding sediments, these data indicate a reasonable agreement with first order kinetics, although an important variability exists from sediment to sediment (fig. 4). From these data, a value of about 3×10^{-8} sec^{-1} (range $2\text{-}7 \times 10^{-8}$ sec^{-1}) can be deduced as a reasonable estimate for k_a.

Nitrification Rate within the Nitrification Layer

In the preceding model, nitrification rate was considered as an independent parameter. Of course, this is not quite correct, because nitrification is limited by ammonium availability.

Direct measurements of nitrification rate in the upper layer of the sediments from the Southern Bight of the North Sea (Billen, 1978) show indeed that it is closely related to the rate of ammonification (fig. 5). In

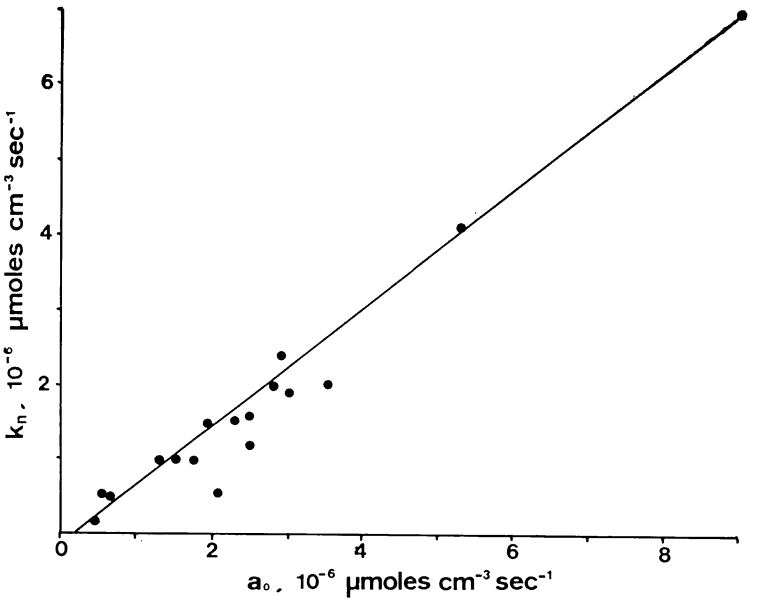

Fig. 5. Relation between nitrification rate and ammonification rate in the top layer of the sediments from the Southern Bight of the North Sea.

the general model, the easiest way for taking into account the limitation of nitrification by ammonium production is to consider k_n as proportional, at any depth within the nitrification layer, to the rate of ammonification:

$$k_n(z) = \gamma \cdot k_a\, C°_{orgN}\, e^{-\alpha z} = k°_n\, e^{-\alpha z} \tag{12}$$

with

$\gamma = 0.8$ (see fig. 5)

$k°_n = \gamma k_a\, C°_{orgN}$

This modifies the solutions of eqs (5) and (10). Solution of eq (5) becomes:

$$\left.\begin{aligned} C_{NO_3} &= \frac{k°_n}{\alpha^2 D_i}\,[1 - e^{-\alpha z}] + Az + C°_{NO_3} && \text{for } z \leqslant z_n \\ C_{NO_3} &= C_{NO_3}(z_n)\, e^{-\sqrt{\frac{k_d}{D_i}}\,[z - z_n]} && \text{for } z \geqslant z_n \end{aligned}\right\} \tag{13}$$

Continuity of the derivatives at $z = z_n$ gives:

$$A = \frac{-1}{1 + z_n \sqrt{\frac{k_d}{D_i}}} \left[\sqrt{\frac{k_d}{D_i}}\,(C°_{NO_3} + \frac{k°_n}{\alpha^2 D_i}\,(1 - e^{-\alpha z_n})) + \frac{k°_n}{\alpha D_i}\, e^{-\alpha z_n} \right] \tag{14}$$

The diffusive flux of nitrate across the sediment water interface can be calculated by the relation:

$$J°_{NO_3} = -D_i \left[\frac{dC_{NO_3}}{dz}\right]_{z=0} = -\frac{k°_n}{\alpha} - D_i A \tag{15}$$

Integrated rates of nitrification (I_{nitr}) and of denitrification (I_{denitr}) are given by:

$$I_{nitr} = \int_0^{z_n} k°_n\, e^{-\alpha z} dz = -\frac{k_n{}^0}{\alpha}\,[1 - e^{\alpha z_n}] \tag{16}$$

$$I_{denitr} = D_i \left[\frac{dC_{NO_3}}{dz}\right]_{z_n} = -\frac{k_n{}^0}{\alpha}\, e^{-\alpha z_n} - D_i A \tag{17}$$

On the other hand, the solution of eq (10) becomes:

$$\left.\begin{aligned} C_{NH_4} &= \frac{a_o}{\alpha^2}\,[1 - \gamma]\,[1 - e^{-\alpha z}] + \gamma \frac{a_o}{\alpha}\, e^{-\alpha z_n} \cdot z && \text{for } z \leqslant z_n \\ C_{NH_4} &= C_{NH_4}[z_n] + \frac{a_o}{\alpha^2}\,[e^{-\alpha z_n} - e^{-\alpha z}] && \text{for } z \geqslant z_n \end{aligned}\right\} \tag{18}$$

where $a_o = k_a\, C°_{orgN}$ and the flux of ammonium to the overlying water is given by

$$J°_{NH_4{}^+} = -D_i \frac{a_o}{\alpha}\,[1 - \gamma + \gamma e^{-\alpha z_n}] \tag{19}$$

The Redox Model

The depth of the nitrification layer (z_n) depends on the redox conditions prevailing in the sediments. Previous work has shown that a critical Eh value exists below which nitrification stops and denitrification starts (Billen, 1975).

For calculating z_n, a complete balance of oxidant consumption must be made up so that the redox profile within the sediment can be calculated.

A simplified, equilibrium model of redox profile in sediments has been presented elsewhere (Billen and Verbeustel, 1980). This model however was based on complete internal thermodynamic equilibrium, including nitrogen species, which is rather unrealistic (Billen, 1975). Moreover, this model considered only one mixing coefficient both for solid and dissolved species. An improved version of this redox model will therefore be presented here. Although it is not really necessary in the scope of a model of nitrogen recycling, the redox model will be presented in a quite general form and will include the processes of sulfate reduction and methane production. However, among the possible results of the model, only those directly related to nitrogen recycling will be discussed in this paper. Other applications will be published elsewhere.

The general principles of the model can be summarized as follows: organic matter degradation by organotrophic microorganisms generates a flux of electrons to the chemical system formed by the mineral redox couples susceptible to be used as electron acceptors in microbial respiration. This happens directly, in the case of respiratory metabolism or indirectly in the case of fermentative metabolism, the reduced products of which are further oxidized by respirative organisms. The oxidants absorbing the flux of electron generated by organic matter degradation are those of the redox couples O_2/H_2O; Mn^{IV}/Mn^{II}; $NO_3/N_2/NH_4^+$; Fe^{III}/Fe^{II}; $SO_4^=/HS^-$; CO_2/CH_4. If it is assumed that an internal thermodynamic equilibrium exists between all these species (nitrogen forms excepted), their depth distribution, and the vertical profile of redox potential (Eh), can be calculated from the vertical profile of organotrophic activity and the knowledge of the mixing properties within the sediment.

Let C_{Ox_j} stand for the concentration of oxidant j (in moles/dm^3 sediment). At steady state, the following diagenetic equation can be written, again neglecting the processes of adsorption, compaction, and sedimentation:

$$O = D_j \frac{d^2 C_{Ox_j}}{dz^2} + p_j - c_j \qquad (20)$$

where p_j and c_j are the rate of production and consumption of oxidant j, and D_j is either D_s or D_i according to the solid or dissolved nature of Ox_j.

Summing up this diagenetic equation for each oxidant multiplied by a coefficient ν_j, corresponding to the number of electrons accepted by it upon being reduced, yields:

$$\sum_j D_j \nu_j \frac{d^2 C_{Ox_j}}{dz^2} + \sum_j [\nu_j p_j - \nu_j c_j] = 0 \qquad (21)$$

This equation expresses the redox balance (in electron equivalents) at each depth in the sedimentary column. The second term represents the overall rate of oxidant consumption and production due to organotrophic activity. As a matter of fact, this process, not only causes a direct flux of electron to the oxidants but also produces carbonate which is a potential oxidant for respiratory metabolisms. If the following stoichiometry is supposed to represent the process of organic matter degradation:

$$C_{org} \rightarrow HCO_3^- + 4e^-$$

The second term of eq (21) can be written

$$\sum_j [\nu_j p_j - \nu_j c_j] = -4\, R(z) + \nu_{HCO_3^-} \cdot R(z) \qquad (22)$$

where R(z) is the rate of organic carbon degradation and $\nu_{HCO_3^-}$ is the number of electrons accepted by carbonate when used in a respiratory metabolism. The reduced product formed under this circumstance being methane, $\nu_{HCO_3^-}$ is equal to 8. As R(z) can be written $k_a\, C^\circ_{org}\, e^{-\alpha z}$ according to the simplified first order (one G) model explained above, eq (21) can be rewritten in the following way:

$$\sum_j D_j \nu_j \frac{d^2 C_{Ox_j}}{dz^2} + 4\, k_a C^\circ_{org}\, e^{-\alpha z} = 0 \qquad (23)$$

With the following boundary conditions:

$$\sum_j D_j \nu_j C_{Ox_j} = \sum_j D_j \nu_j C_{Ox_j}^{\,0} \qquad \text{for } z = 0$$

and

$$\sum_j D_j \nu_j \frac{dC_{Ox_j}}{dz} = 0 \qquad \text{for } z = \infty,$$

The solution of eq (23) is

$$\sum_j D_j \nu_j C_{Ox_j} = \sum_j D_j \nu_j C_{Ox_j}^{\,0} + \frac{4\, k_a C_{org}}{\alpha^2} [1 - e^{-\alpha z}] \qquad (24)$$

The C_j must now be expressed as functions of Eh, by using the hypothesis of internal thermodynamic equilibrium, in the system O_2/H_2O; Mn^{IV}/Mn^{II}; Fe^{III}/Fe^{II}; $SO_4^=/HS^-$; CO_2/CH_4. The reactions considered between these species will be discussed in turn.

Unless explicitly mentioned, thermodynamic data used for calculating the equilibrium relationship are those quoted by Garrels and Christ (1965). Apparent activity coefficients in seawater are taken from Smith (1974).

1. *Oxygen.*—The control of redox potential by oxygen in natural aerated waters has been discussed in detail by Sato (1960) and Breck (1972). Both authors suggested that the effective Eh control in aerated waters results from the rapid and reversible equilibrium between oxygen and hydrogen peroxide,

$$O_2 + 2H^+ + 2e^- \rightleftharpoons H_2O_2$$

rather than the complete and very slow interconvertion between oxygen and water $O_2 + 4e^- + 4H^+ \rightleftharpoons 2H_2O$. The operational relationship between oxygen partial pressure and Eh proposed by Breck (1972):

$$Eh = 1.012 - 0.059\ pH + 0.030 \log pO_2 \tag{25}$$

has been shown to explain quite accurately the behavior of manganese in the Scheldt Estuary (Wollast, Billen, and Duinker, 1979) and will be used here. Taking into account the value of 230μM for oxygen solubility in seawater at 20°C (Strickland and Parsons, 1968) and considering a constant value of pH = 7.5, relation (25) can be written:

$$C_{O_2} = \phi m_{O_2} = \phi\ 10^{\frac{E-0.658}{0.03}} \tag{26}$$

where ϕ is the porosity of the sediment considered, close to 0.5 in sands.

2. *Manganese.*—The redox behavior of manganese in natural environments results from the existence of two solid phases: MnO_2 (and other manganese oxides and hydrous oxides which will not be considered here), stable at high Eh and poorly soluble, and $MnCO_3$ stable at lower Eh and much more soluble (Hem, 1963; Morgan, 1966; Crerar and Barnes, 1974; Wollast, Billen, and Duinker, 1979). Taking into account the thermodynamical data quoted by Morgan (1966), the following equilibrium relations can be written at pH 7.5:

in the field of MnO_2 stability:

$$\begin{aligned} &MnO_2 + 2e^- + 4H^+ \rightleftharpoons Mn^{++} + 2H_2O \\ &Eh = 0.364 - 0.030 \log m_{Mn^{++}} \end{aligned} \tag{27}$$

in the field of $MnCO_3$ stability:

$$\begin{aligned} &Mn^{++} + HCO_3^- \rightleftharpoons MnCO_3 + H^+ \\ &\log m_{Mn^{++}} = -6.9 - \log m_{HCO_3^-} \end{aligned} \tag{28}$$

The transition between the two solid phases occurs at

$$Eh_{MnO_2} = 0.572 + 0.03 \log m_{HCO_3^-} \tag{29}$$

If steady state diagenetic equations similar to eq (20) are written for each of the three manganese species (MnO_2, $MnCO_3$, Mn^{++}) and are summed up, mass conservation implies that

$$D_s \frac{d^2C_{MnO_2}}{dz^2} + D_s \frac{d^2C_{MnCO_3}}{dz^2} + D_i \frac{d^2C_{Mn^{++}}}{dz^2} = 0 \tag{30}$$

where C refers, as above, to the concentration expressed per unit sediment volume.

With the following boundary conditions:

$$C_{MnO_2} + C_{MnCO_3} + \frac{D_i}{D_s} C_{Mn^{++}} = M_o \qquad \text{at } z = 0$$

and

$$\frac{d}{dz}\left[C_{MnO_2} + C_{MnCO_3} + \frac{D_i}{D_s} C_{Mn^{++}} \right] = 0 \qquad \text{at } z = \infty ,$$

the solution of eq (30) is

$$C_{MnO_2} + C_{MnCO_3} + \frac{D_i}{D_s} C_{Mn^{++}} = M_o \tag{31}$$

Combining (31) with (27) and (29) gives:

$$\left.\begin{aligned} C_{MnO_2} &= M_o - \left[\frac{D_i}{D_s} - 1 \right] \phi \, 10^{\frac{-Eh+0.364}{0.030}} && \text{for } Eh > Eh_{MnO_2} \\ C_{MnO_2} &= 0 && \text{for } Eh < Eh_{MnO_2} \end{aligned}\right\} \tag{32}$$

With a good approximation, M_o represents the manganese content of the uppermost sediment layer (where $Eh >> 0.364$ mV). This is about 40 mmoles dm^{-3} in the sediments of the North Sea (Wollast, 1976).

3. *Iron.*—The redox behavior of iron is best described by considering some metastable but reactive solid phases instead of the true thermodynamically stable ones which are only very slowly formed from the former. This is the reason why we considered "amorphous ferric hydroxide" [$Fe(OH)_3$] instead of hematite in oxidized environments (Garrels and Christ, 1965) and mackinawite [FeS] instead of pyrite in reduced ones (Berner, 1967; Doyle, 1968). For the sake of simplicity siderite [$FeCO_3$] is considered as the only stable solid phase at intermediate Eh, although vivianite or glauconite could also appear (Berner, 1971; Bricker and Troup, 1975).

Taking into account the thermodynamic data and the activity coefficient mentioned above, the following equilibrium relationships between these solid phases and dissolved Fe^{++} can be written:

in the stability field of $Fe(OH)_3$:

$$Fe(OH)_3 + 1e^- + 3H^+ \rightleftharpoons Fe^{++} + 3H_2O$$
$$Eh = -0.229 - 0.059 \log m_{Fe^{++}} \quad (33)$$

in the stability field of $FeCO_3$

$$Fe^{++} + HCO_3^- \rightleftharpoons FeCO_3 + H^+$$
$$\log m_{Fe^{++}} = -6.86 - \log m_{HCO_3^-} \quad (34)$$

The frontier between these two solid phases corresponds to

$$Eh = Eh_{Fe(OH)_3} \equiv 0.176 + 0.059 \log m_{HCO_3^-} \quad (35)$$

The equilibrium relationships involving FeS will be discussed below. The same line of argument as for manganese allows me to write:

$$C_{Fe(OH)_3} + C_{FeCO_3} + C_{FeS} + \frac{D_i}{D_s} C_{Fe^{++}} = I_o \quad (36)$$

$$\left.\begin{aligned} C_{Fe(OH)_3} &= I_o - \left[\frac{D_i}{D_s} - 1\right] \phi \; 10^{\left[\frac{-Eh+0.229}{0.059}\right]} \quad \text{for } Eh > Eh_{Fe(OH)_3} \\ \text{and} \\ C_{Fe(OH)_3} &= 0 \qquad\qquad\qquad\qquad\qquad\qquad \text{for } Eh < Eh_{Fe(OH)_3} \end{aligned}\right\} \quad (37)$$

where I_o represents the iron content of the uppermost sediment layer, close to 200 mmoles/dm³ in the sediments of the North Sea (Wollast, 1976).

4. *Sulfate and sulfide.*—In the presence of $FeCO_3$, reduction of sulfate results in FeS production, according to the reaction:

$$SO_4^= + FeCO_3 + 9H^+ + 8e^- \rightleftharpoons FeS + HCO_3^- + 4H_2O$$

for which, the following equilibrium relation can be written at pH 7.5

$$Eh = -0.219 - 0.007 \log m_{HCO_3^-} + 0.007 \log m_{SO_4^=} \quad (38)$$

Free dissolved sulfide concentration remains quite low as long as $FeCO_3$ is still present, as shown by the equilibrium relation for the reaction $HS^- + FeCO_3 \rightleftharpoons FeS + HCO_3^-$

$$m_{HS^-} = m_{HCO_3^-} \cdot 10^{-4.15} \quad (39)$$

It rises, however, once all available siderite has been converted into mackinawite; the equilibrium relation for sulfate conversion into sulfide by the reaction $SO_4^= + 8e^- + 9H^+ \rightleftharpoons HS^- + 4H_2O$ is then at pH 7.5

$$Eh = -0.252 + 0.007 \log \frac{m_{SO_4^=}}{m_{HS^-}} \quad (40)$$

On the other hand, mass conservation of sulfur species implies that

$$D_i \frac{d^2C_{SO_4^=}}{dz^2} + D_s \frac{dC_{FeS}}{dz^2} + D_i \frac{d^2C_{HS^-}}{dz^2} = 0$$

As above, the solution of this differential equation is

$$C_{SO_4^=} + C_{HS^-} + \frac{D_s}{D_i} C_{FeS} = S_o \tag{41}$$

where S_o is the sulfate concentration, expressed per dm^3 sediment, in the uppermost layer. Considering a concentration of 28 mM sulfate in seawater and a porosity of 0.5, S_o is 14 mmoles/dm^3.

The value of Eh_{FeS} where all available iron is converted into mackinawite and below which free sulfide accumulates can now be calculated by combining (41) and (36):

$$C_{FeS} = \frac{D_i}{D_s} [S_o - C_{SO_4^=} - C_{HS^-}] = I_o \tag{42}$$

Substituting $C_{SO_4^=}$ and C_{HS^-} by their expression in (38) and (39) and rearranging give:

$$Eh_{FeS} = -0.219 + 0.007 \log \left(- \frac{1}{\phi m_{HCO_3^-}} \left[\frac{D_s}{D_i} I_o - S_o + m_{HCO_3^-} \cdot 10^{-4 \cdot 15} \right] \right) \tag{43}$$

From relations (37), (38), (40), (41), and (43), the relation between $C_{SO_4^=}$ and Eh can now be written:

$$\left.\begin{aligned} C_{SO_4^=} &= S_o && \text{for } Eh > Eh_{Fe(OH)_3} \\ C_{SO_4^=} &= \phi\, m_{HCO_3}\, 10^{\left[\frac{Eh+0.219}{0.007}\right]} && \text{for } Eh < Eh_{Fe(OH)_3} \\ & && \quad > Eh_{FeS} \\ C_{SO_4^=} &= \frac{\left[S_o - \frac{D_s}{D_i} I_o \right] 10^{\frac{Eh+0.252}{0.007}}}{1 + 10^{\frac{Eh+0.252}{0.007}}} && \text{for } Eh < Eh_{FeS} \end{aligned}\right\} \tag{44}$$

5. *Carbonate and methane.*—The equilibrium relationship for bicarbonate reduction to methane:

$$HCO_3^- + 8e^- + 9H^+ \rightleftharpoons CH_4 + 3H_2O$$

can be written in the following way, if a value of 1 mM for methane solubility in shallow sea water at 20°C is assumed, as done by Martens and Berner (1977):

$$Eh = -0.293 + 0.007 \log \frac{m_{HCO_3^-}}{m_{CH_4}} \tag{45}$$

On the other hand, neglecting the processes of carbonate precipitation or redissolution (which is reasonable for terrigenous sands), considering only dispersive transport for methane (no bubble formation),

and taking into account CO_2 formation associated with organic matter degradation, the following mass balance equation can be written:

$$D_i \frac{d^2C_{HCO_3^-}}{dz^2} + D_i \frac{d^2C_{CH_4}}{dz^2} + k_a C^\circ_{org} e^{-\alpha z} = 0 \qquad (46)$$

With the following boundary conditions:

$$C_{HCO_3} + C_{CH_4} = B_o \qquad \text{for } z = 0$$

where B_o is the bicarbonate content of sediment in the uppermost layer, about 1 mmole/dm^3 in North Sea sediment.

$$\frac{d[C_{HCO_3} + C_{CH_4}]}{dt} = 0 \qquad \text{for } z = \infty$$

The solution of (46) is

$$C_{HCO_4^-} + C_{CH_4} = B_o + \frac{k_a C^\circ_{org}}{\alpha^2 D_i} [1 - e^{-\alpha z}] \qquad (47)$$

From relations (45) and (47), it follows that

$$C_{HCO_3^-} = \frac{10^{\frac{Eh+0.293}{0.007}} \left[B_o + \frac{k_a C^\circ_{org}}{\alpha^2 D_i} (1 - e^{-\alpha z}) \right]}{1 + 10^{\frac{Eh+0.293}{0.007}}} \qquad (48)$$

6. *Nitrate.*—Nitrate is not considered to be at equilibrium with respect to the other oxidants; its behavior is simply described by eq (13) above.

Owing to relations (26), (32), (37), (44), (48), and (13), the concentration C_{Ox_j} of all oxidants (O_2, MnO_2, $Fe(OH)_3$, $SO_4^=$, HCO_3^-, and NO_3^- respectively) can now be expressed as functions of z and Eh. Introducing these functions in relation (23) provides an implicit relation between Eh and z, of the form

$$f(Eh, z, z_n, k_d) = 0 \qquad (49)$$

This relation still contains two undefined parameters, z_n and k_d, that have to be determined.

The value of k_d depends on the overall rate of oxidants consumption by organotrophic activity at depth z_n. At this particular depth, the electron flux generated by organic matter degradation is entirely absorbed by nitrate reduction. k_d can therefore be defined as

$$k_d = \frac{4k_a C^\circ_{org}}{5} e^{-\alpha z_n} \cdot \frac{1}{C_{NO_3(z_n)}} \qquad (50)$$

z_n, on the other hand, is defined as the depth at which the redox potential reaches the critical value of 0.327 mV below which ammonium oxidation

is no more exoenergetic, nitrification can no longer proceed, and denitrification starts. For this particular value of Eh, eq (49) can be written:

$$f(z_n) = 0 \tag{51}$$

z_n can then be determined by looking for the zero of this function. Knowing the value of z_n, relation (49) can be used for determining the complete redox profile in the sediment.

Summary of the Model

The general model of nitrogen recycling just described can be used, as was intended, for calculating the fluxes of ammonium and nitrate

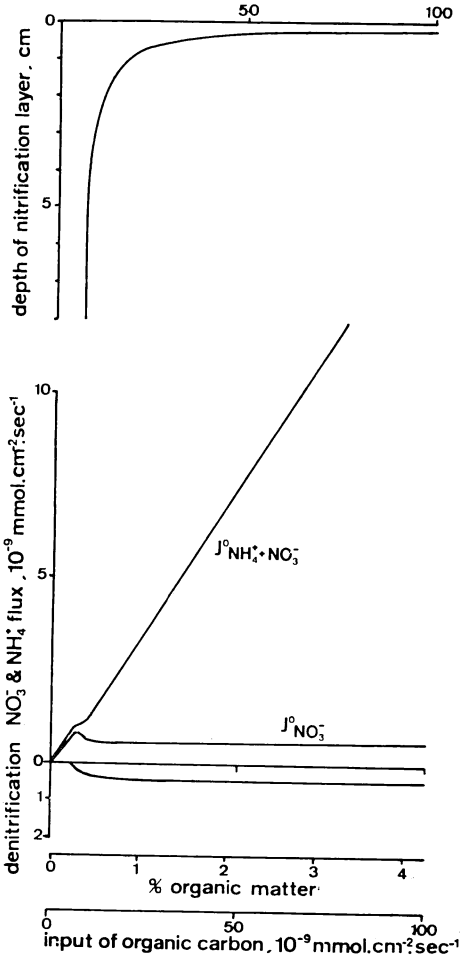

Fig. 6. Mean organic matter content of the uppermost 1 cm sediment layer, ammonium and nitrate flux to the overlying water, denitrification rate and depth of the nitrification layer as a function of the input of organic matter to the sediments, calculated with the model described in the text for the following values of the parameters: $D_1 = 10^{-4}$ cm^2 sec^{-1}; $D_s = 10^{-7}$ cm^2 sec^{-1}; $k_a = 3\ 10^{-8}$ sec^{-1}, = 6, = 0.8; $C_{NO_3}^{\circ}$ = 0 mmoles cm^{-3}.

nitrogen recycled to the water column and the total rate of denitrification as functions of the amount of organic matter sedimenting, given the C/N ratio of this material and the mixing coefficient of the solid and dissolved phases of the sediment.

Following is the procedure: for each chosen value of the flux of sedimenting organic matter ($J°_{org}$), it is possible to calculate successively,

1. The organic carbon and nitrogen content ($C°_{orgC}$ and $C°_{orgN}$) of the uppermost layer of the sediment (relation 3).
2. The rates of organotrophic activity ($k_a\ C°_{orgC}\ e^{-\alpha z}$) and of ammonification ($k_a\ C°_{orgN}\ e^{-\alpha z}$), the rate of nitrification in the nitrification layer (relation 12), the depth of the nitrification layer (relation 15), and, if wanted, the whole redox profile (relation 49).

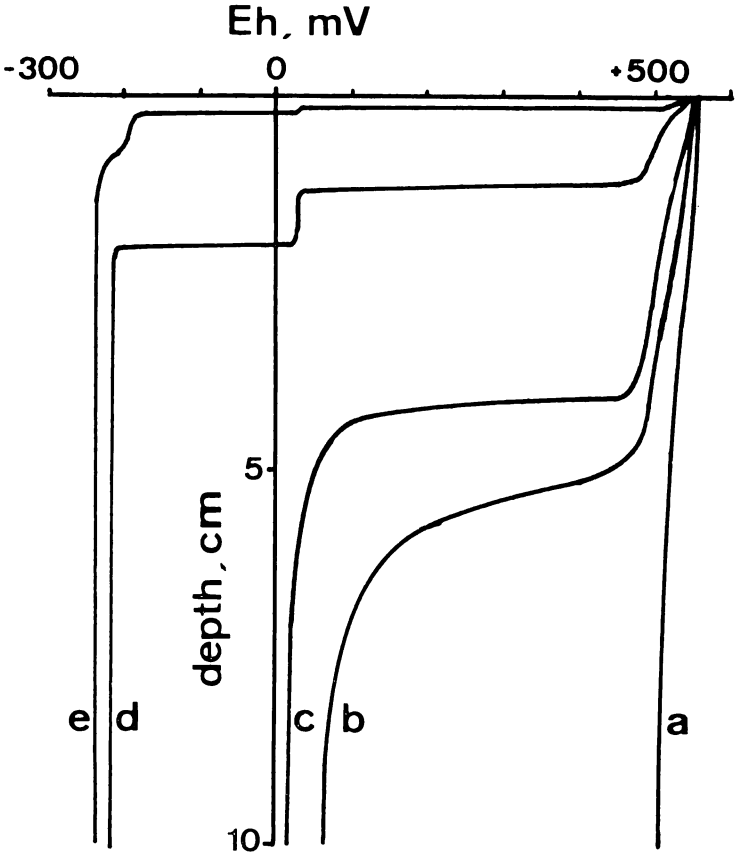

Fig. 7. Vertical profiles of redox potential in sediments, as calculated with the model for the values of the parameters listed in figure 6 and at the following values of the flux of organic carbon to the sediment: (a.) 5 10^{-9} mmoles C cm^{-2} sec^{-1}; (b.) 7.5 10^{-9} mmoles C cm^{-2} sec^{-1}; (c.) 8 10^{-9} mmoles C cm^{-2} sec^{-1}; (d.) 15 10^{-9} mmoles C cm^{-2} sec^{-1}; (e.) 100 10^{-9} mmoles C cm^{-2} sec^{-1}.

3. The values of the fluxes of ammonium and nitrate across the sediment interface (relation 19 and 15) and the integrated value of denitrification (relation 17).

All calculations can be performed with a simple programmable pocket calculator.

RESULTS AND DISCUSSION OF THE MODEL

Figure 6 shows the results of the calculation of the depth of the nitrification layer, of the ammonium and nitrate fluxes across the sediment water interface, and of the integrated rate of denitrification as a function of the input of organic carbon to the bottom, according to the model presented above, for values of the parameters D_s, D_i, k_a, γ, and β representative of North Sea sandy sediments as discussed above.

Also shown is the value of the mean organic matter content of the 1 cm thick upper sediment layer, calculated as

$$\overline{C_{orgC}} = \frac{1}{1\,cm}\int_0^{1\,cm} C^\circ_{orgC}\, e^{-\alpha z}\, dz = C^\circ_{orgC} \cdot \left[\frac{1-e^{-\alpha}}{\alpha}\right] \qquad (52)$$

Figure 7 shows the entire vertical redox profiles for several values of the input of organic carbon to the sediment and the same values of the parameters.

The sensitivity of the results toward the values of the parameters can be appreciated from figure 8 showing the results of the calculation of nitrate flux and integrated denitrification for different values of the parameters D_s, D_i, and k_a. It is seen that a fifty-fold variation of D_s results only in a two-fold variation in nitrate recycling and denitrification rate. The sensitivity toward D_i and k_a is a little more important. However, the

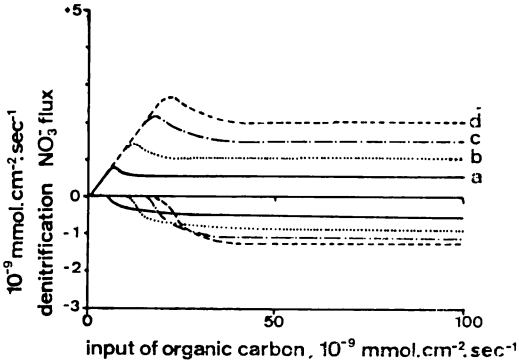

Fig. 8. Nitrate flux to the overlying water and denitrification calculated for different values of the parameters:

(a) $D_i = 10^{-4}$ cm²sec⁻¹ ; $D_s = 10^{-7}$ cm²sec⁻¹ ; $k_a = 3\,10^{-8}$ sec⁻¹
(b) $D_i = 2\,10^{-4}$ " ; $D_s = 10^{-7}$ " ; $k_a = 3\,10^{-8}$ "
(c) $D_i = 10^{-4}$ " ; $D_s = 10^{-8}$ " ; $k_a = 3\,10^{-9}$ "
(d) $D_i = 10^{-4}$ " ; $D_s = 10^{-7}$ " ; $k_a = 10\,10^{-8}$ ".

Other parameters as in figure 6.

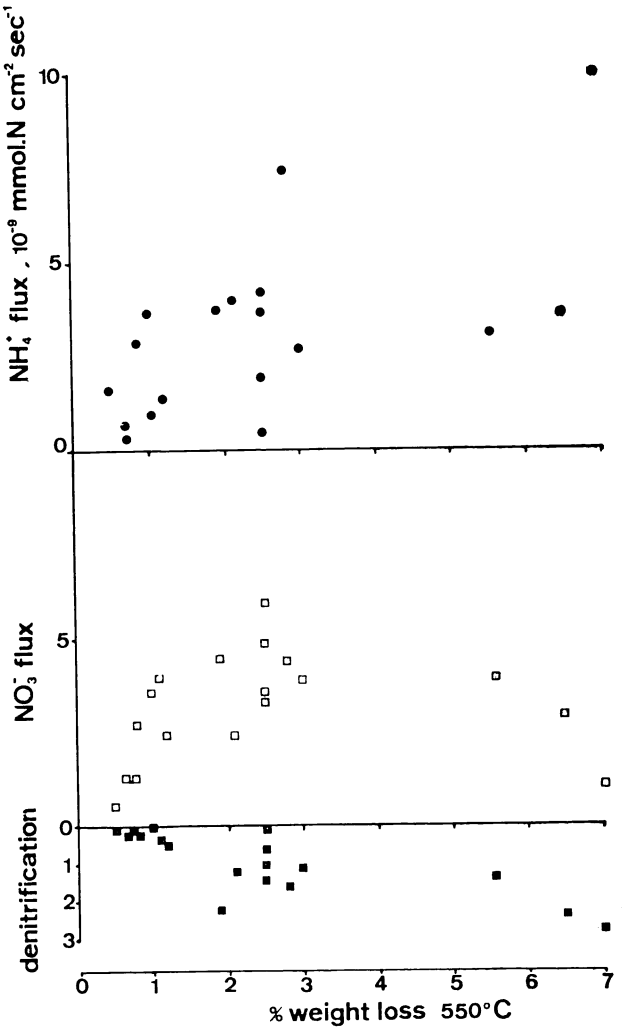

Fig. 9. Ammonium and nitrate flux to the overlying water and denitrification rate, estimated on several cores from the Southern Bight of the North Sea, off the Belgian coast, and plotted as a function of the organic matter content of the top layer of the sediments (data from Billen, 1978).

general trends of variation of the processes, under the effect of an increased flux of organic matter depositing, are quite similar whatever the value of the parameters.

At least as far as these general trends are concerned, the predictions of the model compare well with the empirical data obtained by individual analysis of depth distribution of ammonium and nitrate on cores collected in the Southern Bight of the North Sea (Billen, 1978). These data are plotted in figure 9 as a function of organic matter content of the upper sediment layer, on a format similar to that of figure 6 and 8. The idealized model of course does not intend to predict accurately the absolute value of the recycling fluxes for any sedimentary environment. Too many parameters are involved, and their variability, even in a single environment, is too large for this. Instead, the usefulness of the model lies in predicting the trends of the variations of the relative values of nutrient fluxes as the result of variations of organic matter input.

These trends can be summarized in the following way: (1) At low input of organic material to the sediment, most of nitrogen recycling occurs as nitrate. With increasing input of organic matter, the part of ammonium release becomes more important, while nitrate recycling

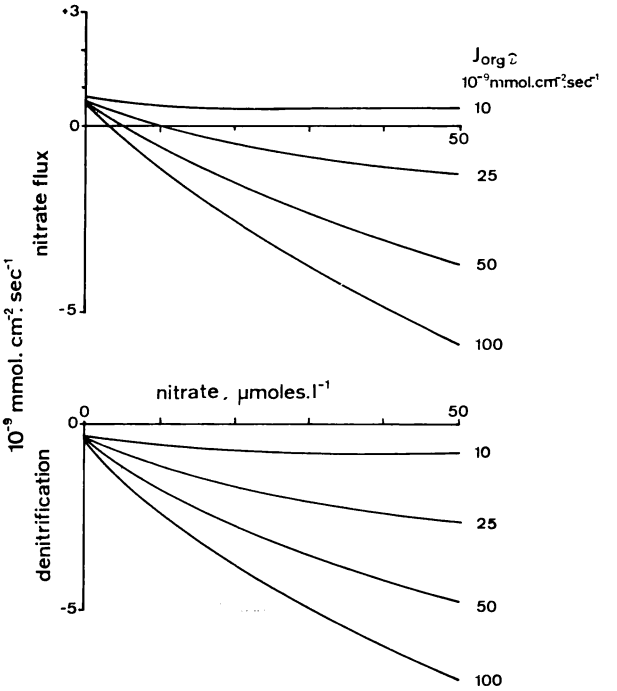

Fig. 10. Effect of nitrate concentration in the overlying water on the flux of nitrate across the sediment-water interface and on the rate of denitrification, calculated with the model described for the same values of the parameters as in figure 6, and for various values of the flux of depositing organic material ($J°_{org}$), indicated in 10^{-9} mmoles cm^{-2} sec^{-1}.

TABLE 2

Measured values of integrated denitrification rates in sedimentary environments

Location		Nitrate concentration in the overlying water μmole/l	Integrated rate of denitrification 10^{-6} mmoles N $cm^{-2}sec^{-1}$	Method	Authors
Coastal North Sea	summer	2	1.1	mathematical analysis of pore water concentration profiles	Billen, 1978
		2	1.6		
	winter	10	1.4		
		20	2.25		
Salt Marsh eastern USA coast —(groundwater NO_3 imports)			8-10	measurements of N_2 net release	Kaplan, Valiela, and Teal, 1979
Bering Sea		5-15	0.25	^{15}N-tracer method	Koide and Hattori, 1979
Arresø lake (DK) (anunal mean)		0-100	0.29	^{15}N-tracer method	Pheiffer-Madsen, 1979
Randers Fjord (DK)	winter	125	1.1	Acetylene inhibition technique	Sørensen, 1978
	winter	60	1.0		Sørensen, Jørgensen, and Revsbech, 1979
	summer	≅0	0.14		
Kysing Fjord (DK)	winter	75	3.0		
	summer		0.02		
	October	3.4	0.19	^{15}N-tracer method	Oren and Blackburn, 1979
Narragansett Bay (USA)	summer	0.2-3.3	2.7	measurement of N_2 net release	Seitzinger and others, 1982

reaches a maximum. Ammonium recycling prevails at high organic input. (2) Denitrification, being dependent on nitrate formed by nitrification in the nitrification layer, reaches also a plateau above a certain input of organic material. This implies that the relative value of denitrification in the overall nitrogen cycle is maximum at an intermediate input of depositing material and decreases at higher inputs. Because denitrification mostly results in producing of flux of N_2 to the water column (although some N_2O and NH_4^+ can also be produced, Sørensen, 1978; Firestone and Tiedje, 1979), it can be considered as causing a net loss of nitrogen from the ecosystem. In the absence of nitrate in the overlying water, this loss is not expected to concern more than about 30 percent of of the flux of nitrogen remineralized. Only when high nitrate concentrations exist in the overlying water, more important denitrification rates can occur, with the sediment acting as a sink for nitrates from the water column (fig. 10). This effect of high nitrate concentration in the overlying water on the rate of denitrification in the sediment is much more pronounced, however, at high organic content of the sediment (that is, at high organic flux to the sediment) than for organic poor sediments (fig. 10).

This conclusion is concordant with observed values of denitrification rates in various sedimentary environments, reported in the literature (see table 2). The range of most of these measurements is $0 - 30 \times 10^{-9}$ mmoles cm^{-2} sec^{-1}, in good agreement with the values predicted by the model (see fig. 8). The highest values generally correspond to environments where high nitrate exists in the overlying water. Only Kaplan, Valiela, and Teal (1979) found denitrification rates as high as $8 - 10 \times 10^{-9}$ mmoles cm^{-2} sec^{-1}, in a salt march ecosystem receiving large import of NO_3^- through ground water.

It must be stressed once more that the model presented here is an idealized one. Important simplifying assumptions have been made, which limit the general validity of its quantitative conclusions. One of the most important simplifications consists in considering constant values of the mixing coefficients D_s and D_i over the entire depth interval considered. Because of this, the model is only valid in the upper bioturbated layer of sediments. As already shown above (see table 1), this layer extends down 15 to 20 cm in sandy sediments but is often restricted to a few cm in muds. In the latter case, the processes occuring below the bioturbation layer can be predominant in organic matter degradation and nutrient recycling.

For this reason, and also because it does not take into account adsorption processes, the model presented applies better to sandy than to muddy sediments. The model also assumes a constant value of k_a with depth, considering that all biodegradable organic matter has the same first order degradation rate constant. As said above, a "multi-G model" (Jørgensen, 1978; Berner, 1980b) taking into account several types of organic material undergoing decomposition with different rate constants should better simulate organotrophic activities in the deeper layers of the sediments but would greatly complicate the calculations. For this reason

also, the model applies better to the top 10 to 20 cm depth interval of the sedimentary column.

Another simplification in the model consists in assuming steady-state. This assumption is only valid if the characteristic time of variations of the parameters is longer than the turnover time of the various compartments. The longest turnover time in the sedimentary system is that of particulate organic nitrogen, which is given by the reciprocal of k_a, that is, about 1 yr. Therefore, the model cannot be used for predicting the response to seasonal variations in the rate of organic matter deposition; however, it can be useful for the prediction of long term effects of modifications in the total input of organic matter to sediments, as occurs for instance during the process of eutrophication.

ACKNOWLEDGMENTS

A first version of this paper was presented at the conference on C, N, and S cycling in sediments held at Sandbjerg Slot, Sønderborg (Denmark) in April 1980. The present version has been considerably amended as a result of the discussion at this conference. The author wishes to express his gratefulness to all the participants of this conference and to the organizers, T. Henry Blackburn, Bo Barker Jørgensen, Jan Sørensen, and Tom Fenchel. He is also grateful to Robert A. Berner, Joseph T. Westrich, and Robert C. Aller for valuable comments on an earlier version of the manuscript.

REFERENCES

Aller, R. C., 1978, Experimental studies of changes produced by deposit feeders on pore water, sediment and overlying water chemistry: Am. Jour. Sci., v. 278, p. 1185-1234.

Aller, R. C., Benninger, L. K., and Cochran, J. K., 1980, Tracking particle-associated processes in nearshore environment by use of $^{234}Th/^{238}U$ dis-equilibrium: Earth Planetary Sci. Letters, v. 47, p. 161-175.

Aller, R. C., and Cochran, J. K., 1976, $^{234}Th/^{238}U$ disequilibrium in nearshore sediment: particle reworking and diagenetic time scales: Earth Planetary Sci. Letters, v. 29, p. 37-50.

Aller, R. C., and Yingst, J. Y., 1980, Relationship between microbial distribution and the anaerobic decomposition of organic matter in surface sediments of Long Island Sound (USA): Marine Biology, v. 56, p. 29-42.

Berger, W. H., and Heath, G. R., 1968, Vertical mixing in pelagic sediments: Jour. Marine Research, v. 26, p. 134-143.

Berner, R. A., 1964, An idealized model of dissolved sulfate distribution in recent sediments: Geochim. et Cosmochim. Acta, v. 28, p. 1497-1503.

———— 1967, Thermodynamic stability of sedimentary iron sulfides: Am. Jour. Sci., v. 265, p. 773-785.

———— 1971, Principles of chemical sedimentology: New York, McGraw Hill, 240 p.

———— 1974, Kinetic models for the early diagenesis of nitrogen, sulfur, phosphorus and silicon in anoxic marine sediments, *in* Goldberg, E. D., ed., The Sea, v. 5: New York, John Wiley & Sons, p. 427-450.

———— 1980a, Early diagenesis: A theoretical approach: Princeton, N.J., Princeton Univ. Press, 241 p.

———— 1980b, A rate model for organic matter decomposition during bacterial sulfate reduction in marine sediments, *in* Daumas, R., ed., Biogeochemistry of organic matter at the sediment-water interface: Paris, Ed. Centre National Recherche Sci., p. 35-44.

Billen, G., 1975, Nitrification in the Scheldt estuary (Belgium and the Netherlands): Estuarine and Coastal Marine Sci., v. 3, p. 79-89.

———— 1976, A method for evaluating nitrifying activity in sediments by dark ^{14}C-bicarbonate incorporation: Water Research, v. 10, p. 51-57.

———— 1978, A budget of nitrogen recycling in North Sea sediments off the Belgian coast: Estuarine and Coastal Marine Sci., v. 7, p. 127-146.

Billen, G., and Verbeustel, S., 1980, Distribution of microbial metabolisms in natural environments displaying gradients of oxidation reduction conditions, *in* Daumas, R., ed., Biogeochemistry of organic matter at the sediment-water interface: Paris, Ed. Centre Nat. Recherche Sci., p. 291-300.

Breck, W. G., 1972, Redox potentials by equilibration: Jour. Marine Research, v. 30, p. 121-139.

Bricker, O. W., and Troup, B. N., 1975, Sediment-water exchange in Chesapeake Bay, *in* Carpenter, J. H., ed., Estuarine research: Chemistry, Biology and the Estuarine System, v. 1: New York, Academic Press, p. 3-27.

Crerar, D. A., and Barnes, H. L., 1974, Deposition of deep-sea manganese nodules: Geochim. et Cosmochim. Acta, v. 38, p. 279-300.

Doyle, R. W., 1968, Identification and solubility of iron sulfide in anaerobic lake sediment: Am. Jour. Sci., v. 266, p. 980-994.

Duinker, J. C., Wollast, R., and Billen, G., 1979, Behaviour of manganese in the Rhine and the Scheldt estuaries. II. Geochemical cycling: Estuarine and Coastal Marine Sci., v. 9, p. 727-738.

Duursma, E. K., and Gross, M. G., 1971, Marine sediments and radioactivity, in radioactivity in the marine environment: Washington, D.C., Natl. Acad. Sci., p. 147-160.

Fanning, K. A., and Pilson, M. E. Q., 1974, The diffusion of dissolved silica out of deep-sea sediments: Jour. Geophys. Research, v. 79, p. 1293-1297.

Firestone, M. K., and Tiedje, J. M., 1979, Temporal change in nitrous oxide and dinitrogen from denitrification following onset of anaerobiosis: Applied and Environmental Microbiology, v. 38, p. 673-679.

Garrels, R. M., and Christ, C. L., 1965, Solutions, Minerals and equilibrium: New York, Harper and Row.

Goldberg, E. D., and Koide, M., 1962 Geochronological studies on deep-sea sediments by the thorium-ionium method. Geochim. et Cosmochim. Acta, v. 26, p. 417-450.

Goldhaber, M. B., Aller, R. C., Cochran, J. K., Rosenfeld, J., Martens, C. S., and Berner, R. A., 1977, Sulfate reduction diffusion and bioturbation in Long Island Sound sediments: report of the FOAM Group: Am. Jour. Sci., v. 227, p. 193-237.

Guinasso, N. L., and Schink, D. R., 1975, Quantitative estimate of biological mixing rates in abyssal sediments: Jour. Geophys. Research, v. 80, p. 3032-3043.

Hem, J. D., 1963, Chemical equilibria and rates of manganese oxidation: U.S. Geol. Survey, Water Supply Paper, 1667-1, A1-A64.

Imboden, D. M., 1975, Interstitial transport of solutes in non-steady state accumulating and compacting sediments: Earth Planetary Sci. Letters, v. 27, p. 221-228.

Jørgensen, B. B., 1978, A comparison of methods for the quantification of bacterial sulfate reduction in coastal marine sediments. II. Calculation from mathematical models: Geomicrobiology Jour., v. 1, p. 29-47.

Kaplan, W., Valiela, I., and Teal, J. M., 1979, Denitrification in a salt marsh ecosystem: Limnology Oceanography, v. 24, p. 726-734.

Koide, I., and Hattori, A., 1979, Estimation of denitrification in sediments of the Bering Sea shelf: Deep Sea Research, v. 26, p. 409-411.

Krishnaswami, S., Benninger, L. K., Aller, R. C., and Von Damm, K. L., 1980, Atmospherically-derived radionuclides as tracers of sediment mixing and accumulation in near-shore marine and lake sediments: evidence from ^{7}Be, ^{210}Pb and $^{239,240}Pu$: Earth Planetary Sci. Letters, v. 47, p. 307-318.

Lerman, A., 1979, Geochemical Processes: Water and sediment environments: New York, John Wiley & Sons, 481 p.

Luedtke, N. A., and Bender, M. L., 1979, Tracer study of sediment-water interactions in estuaries: Estuarine and Coastal Marine Sci., v. 9, p. 643-651.

McCaffrey, R. J., Myers, A. C., Davey, E., Morrisson, G., Bender, M., Luedtke, N., Cullen, D., Froelich, P., and Klinkhammer, G., 1980, The relation between pore water chemistry and benthic fluxes of nutrients and manganese in Narragansett Bay, Rhode Island: Limnology Oceanography, v. 25, p. 31-44.

McCave, I. N., 1973, Mud in the North Sea, *in* Goldberg, E. D., ed., North Sea Science: Cambridge, Mass., Massachusetts Inst. Technology Press, p. 75-100.

Martens, C., and Berner, R. A., 1977, Interstitial water chemistry of anoxic Long Island Sound sediments. I. Dissolved gases: Limnology Oceanography, v. 22, p. 10-25.

Morgan, J. J., 1966, Chemical equilibria and kinetic properties of manganese in natural waters, *in* Faust, S. D., and Hunter, J., eds., Principles and Applications in Water Chemistry: New York, John Wiley & Sons, p. 561-624.

Nozaki, Y., Cochran, J. K., and Turekian, K. K., 1977, Radiocarbon and ^{210}Pb distribution in submersible-taken deep-sea cores from project famous: Earth Planetary Sci. Letters, v. 34, p. 167-173.

Oren, A., and Blackburn, T. H., 1979, Estimation of sediment denitrification rates at in situ nitrate concentration: Applied and Environmental Microbiology, v. 37, p. 174-176.

Pheiffer-Madsen, P., 1979, Seasonal variation of denitrification rate in sediment determined by use of ^{15}N: Water Research, v. 13, p. 461-465.

Pichot, G., ms, 1980, Simulation du cycle de l'azote à travers l'écosystème pélagique de la baie Sud de la mer du Nord: Thesis, Univ. Liège, Fac. Sci., 168 p.

Robbins, J. A., Krezoski, J. R., and Mozley, S. C., 1977, Radioactivity in sediments of the great lakes: post-depositional redistribution by deposit-feeding organisms: Earth Planetary Sci. Letters, v. 36, p. 325-333.

Rosenfeld, J. K., 1978, Nitrogen diagenesis in Long Island Sound sediments: Am. Jour. Sci., v. 281, p. 436-442.

Rowe, G. T., Clifford, C. H., Smith, K. L., Jr., and Hamilton, P. L., 1975, Benthic nutrient regeneration and its coupling to primary productivity in coastal waters: Nature, v. 255, p. 215-217.

Seitzinger, S., Nixon, S., Pilson, M. E. Q., and Burke, S., 1982, Denitrification and N_2O production in near-shore marine sediments: Geochim. et Cosmochim. Acta, (in press).

Sato, M., 1960, Oxidation of sulfide areas bodies. I. Geochemical environments in terms of Eh and pH: Econ. Geology, v. 55, p. 928-961.

Smith, F. G. W., ed., 1974, Handbook of Marine Science, vol. I: Cleveland, CRC Press.

Sørensen, J., 1978, Denitrification rates in a marine sediment as measured by the acetylene inhibition technique: Applied and Environmental Microbiology, v. 36, p. 139-143.

Sørensen, J., Jørgensen, B. B., and Revsbech, N. P., 1979, A comparison of oxygen, nitrate and sulfate respiration in coastal marine sediments: Microbial Ecology, v. 5, p. 105-115.

Strickland, J. D. J., and Parsons, T. R., 1968, A practical handbook of seawater analysis: Canada Fisheries Research Board Bull., v. 167, p. 1-311.

Vanderborght, J. P., and Billen, G., 1975, Vertical distribution of nitrate in interstitial water of marine sediments with nitrification and denitrification: Limnology Oceanography, v. 20, p. 953-961.

Vanderborght, J. P., Wollast, R., and Billen, G., 1977, Kinetic model of diagenesis in disturbed sediments. I. Mass transfer properties and silica diagenesis: Limnology Oceanography, v. 22, p. 787-793.

Wollast, R., 1976, Propriétés physico-chimiques des sédiments et des suspensions de la mer du Nord, *in* Nihoul, J. C., and Gullentops, F., eds., Modèle Mathématique de la Mer du Nord (Projet Mer), Rapport Final, vol. 4, Sedimentologie. Service du Premier Ministre, Programmation de la Politique Scientifique, p. 139-160.

Wollast, R., Billen, G., and Duinker, J. C., 1979, Behaviour of manganese in the Rhine and Scheldt estuaries. I. Physico-chemical aspects: Estuarine and Coastal Marine Sci., v. 9, p. 161-169.